Published in final edited form as:
Cardiovasc Res. 2012 July 1; 95(1): 108–115. doi:10.1093/cvr/cvs147.

Normal and Abnormal Development of the Intrapericardial Arterial Trunks in Man and Mouse

Robert H. Anderson, BSc, MD, FRCPath[*], **Bill Chaudhry, PhD, MRCP**[*], **Timothy J. Mohun, PhD**[**], **Simon D. Bamforth, PhD**[*], **Darren Hoyland, PhD**[*], **Helen M. Phillips, PhD**[*], **Sandra Webb, PhD**[***], **Antoon F.J. Moorman, PhD**[****], **Nigel A. Brown, PhD**[***], and **Deborah J. Henderson, PhD**[*]

[*]Institute of Genetic Medicine, Newcastle University, UK [**]Division of Developmental Biology, MRC National Institute for Medical Research, London, UK [***]Division of Biomedical Sciences, St George's, University of London, UK [****]Department of Anatomy, Embryology & Physiology, Academic Medical Center, Amsterdam, the Netherlands

Abstract

Aims—The definitive cardiac outflow channels have three components: the intrapericardial arterial trunks; the arterial roots with valves; and the ventricular outflow tracts. We studied the normal and abnormal development of the most distal of these, the arterial trunks, comparing findings in mouse and man.

Methods and Results—Using lineage tracing and three-dimensional visualization by episcopic reconstruction and scanning electron microscopy, we studied embryonic day 9.5 to 12.5 mouse hearts, clarifying the development of the outflow tracts distal to the primordia of the arterial valves. We characterize a transient aortopulmonary foramen, located between the leading edge of a protrusion from the dorsal wall of the aortic sac and the distal margins of the two outflow cushions. The foramen is closed by fusion of the protrusion, with its cap of neural crest cells, with the neural crest cell-filled cushions; the resulting structure then functioning transiently as an aortopulmonary septum. Only subsequent to this closure is it possible to recognize, more proximally, the previously described aortopulmonary septal complex. The adjacent walls of the intrapericardial trunks are derived from the protrusion and distal parts of the outflow cushions, while the lateral walls are formed from intrapericardial extensions of pharyngeal mesenchyme derived from the second heart field.

Conclusions—We provide, for the first time, objective evidence of the mechanisms of closure of an aortopulmonary foramen that exists distally between the lumens of the developing intrapericardial arterial trunks. Our findings provide insights into the formation of aortopulmonary windows and the variants of common arterial trunk.

Address for Communication: Prof Deborah J. Henderson, Institute of Genetic Medicine, Newcastle University, Central Parkway, Newcastle upon Tyne, NE1 3BZ, UK. deborah.henderson@ncl.ac.uk, Tel. +44 191 2418644, FAX: +44 191 2418666.

Disclosures: None

Conflict of Interest: None declared

Europe PMC Funders Author Manuscripts

Keywords

Mouse development; neural crest; second heart field; aortopulmonary window

Introduction

Over the past decade, studies of animal models have transformed our understanding of cardiac embryology. In particular, the use of genetic cell lineage analysis, along with the ability to assess large numbers of specimens, has permitted the accurate tracking of distinct cellular contributions within the developing mouse heart. These findings have provided a framework for understanding cardiac development in man, where comparable studies are hampered by limited availability of specimens, and the impossibility of following cell lineage. As revealed in a recent review by Okamoto and colleagues[1], there are numerous accounts concerning the development of the outflow tract.

Arbitration between the various theories is complicated by the fact that the definitive intrapericardial pulmonary and aortic outflow channels each possess three segments, namely the intrapericardial arterial trunks distal to the sinutubular junctions, the arterial roots with their valves, and the subvalvar ventricular outflow tracts, while development is usually explained in terms of only two components, the truncus and the conus.[2] There is no consensus as to how these two components relate to the three definitive intrapericardial parts of the outflow tracts (OFT), nor the exact temporal and morphologic changes that separate the distal common lumen into the separate intrapericardial aortic and pulmonary trunks. In addition, describing any embryonic structure as an OFT septum is somewhat problematic, given that in the fully-formed heart there is no septum between these two arterial components. It is well established, nonetheless, that during development the aortic and pulmonary channels are separated by mechanisms involving intrapericardial migration of new populations of cells, including those derived from an Islet1-expressing (Isl1) progenitor population in the pharyngeal mesoderm termed the second heart field[3] and neural crest cells (NCC).[4] Using lineage analysis, along with techniques providing three-dimensional visualisations, we have now analysed the contributions made by these populations during separation of the intrapericardial arterial trunks distal to the primordiums of the arterial valves. We have not, in this study, assessed the mechanics of separation of the arterial roots, nor the formation of the subpulmonary infundibulum, although our findings are pertinent to previous studies describing how these components are separated by an aortopulmonary septal complex.[4,5] Subsequent application of our approach to mouse mutants, however, has permitted us to provide mechanistic insights with regard to the morphogenesis of aortopulmonary window and common arterial trunk.

Materials and Methods

(Details and references are provided in supplementary materials)

Mouse and human embryos

We used CD1 (Charles River), Parkes and C57Bl6 mice, employing R26R and R26EYFP reporter lines in combination with the Wnt1-cre and Isl1-cre lines to label permanently NCC and second heart field cells, respectively, as well as Isl1-lacZ mice. Mice were maintained according to the regulations of the UK Home Office and the studies conformed to Directive 2010/63/EU of the European Parliament. We also studied 8 human embryos between Carnegie stages (CS) 13 and 18 obtained from the MRC-Wellcome Human Developmental Biology Resource housed at Newcastle University. Ethical approval for the collection and use of this material was gained from Newcastle University. These studies conformed with the principles outlined in the Declaration of Helsinki.

Histology and immunohistochemistry

Standard protocols were used for staining of paraformaldehyde-fixed embryos. An anti-green fluorescent protein antibody, which also recognizes yellow fluorescent protein, was used to identify positive cells in fixed samples from R26R-EYFP and Isl1-lacZ mice. Xgal staining was used to detect β-galactosidase expression in samples from R26R mice. Each experiment was repeated a minimum of three times, and included appropriate controls.

Three-dimensional reconstruction

Three dimensional reconstructions of 5 serially sectioned staged embryos encompassing embryonic days (E) 9.5 to 12.5 were carried out according to standard protocols. Sections were stained with MF20 antibody to mark the myocardium, and alcian blue to stain the cushion tissue.

Scanning electron microscopy

Embryos from E9.5 through 12.5, using at least 5 embryos for each stage, were cacodylate fixed, dissected and processed by standard techniques to show the salient anatomic features.

High resolution episcopic microscopy

Embryos were prepared and imaged as described in the supplementary materials. We studied 5 datasets from mice at day 10.5, 25 datasets from day 11.5, and 12 datasets from day 12.5. For comparative purposes, we also studied 8 human embryos as already described.

Results

The OFT prior to septation

The cardiac OFT extends from the ventricular mass to the margins of the pericardial cavity. A prominent bend, more acute in human than mouse (compare Figs. 1A and B), initially permits distinction of proximal and distal components. At the margins of the pericardial cavity, the lumen of the OFT is continuous with that of the aortic sac, a manifold embedded within the pharyngeal mesenchyme which gives rise to the pharyngeal arch arteries (Fig. 1D,E). At E9.5 (25 somites, equivalent to CS13 in man), the walls of the OFT are exclusively myocardial (Fig 1C). By early E10.5, the jelly lining the walls is populated by

NCCs, which are contiguous extrapericardially with those forming the walls of the aortic sac and arch arteries (Fig 1C).

By late E10.5 (35 somites, CS14), short non-myocardial spurs are seen cranially and caudally, which indent the myocardial margins towards the ventricles, and express Isl1 (Fig 1D). Initially at E10.5, a prominent mid-sagittal ridge, populated by NCC, separates the right and left sides of the aortic sac between the 3rd and 4th arches (Fig. 1F and Supplementary Fig. 1D). The ridge has attenuated by early E11.5 (not shown), by which time the junction between the OFT and the aortic sac has shifted caudally, so as to lie between the 4th and 6th arches. By this stage, the dorsal wall of the aortic sac has developed a subtle protrusion (arrow in Fig 2A). It is this protrusion, rather than the mid-sagittal ridge, which represents the earliest sign of separation of the cranial aortic and caudal pulmonary channels.

Over the period continuing to late E11.5 (about 50 somites, CS 15), the distal non-myocardial tissue, initially seen cranially and caudally, expands and rotates counterclockwise in ventral view (Compare Figs. 1D, and G, see Supplementary Fig. 2A), producing right-sided and left-sided walls to the outflow tract that are non-myocardial (Supplementary Fig. 2C), and producing a fishmouth configuration for the distal myocardial margins. The myocardial components of the wall now overlie the distal extent of the opposing cushions, which extend proximally throughout the proximal parts of the OFT (Supplementary Fig. 2B,D), while the non-myocardial components overlie the blood-flow channels. The cushion located caudally in the distal part of the OFT terminates proximally on the septal side of the right ventricle (orange in Supplementary Figs. 2&3 and Movie 1), while the second cushion, located cranially in the distal OFT, extends rightwards and parietally, when traced towards the ventricles (yellow in Figures).

Up to the early stage of E11.5, the aortic sac and arch arteries are left-right symmetrical, with the sac giving rise cranially to the 3rd and 4th arch arteries, and caudally to the 6th arch arteries (Fig. 1G,H, Movie 2). By the end of E11.5, and during E12.5, the developing pulmonary arteries have become evident, taking their origin from the mid-ventral portions of the 6th arch arteries (Fig 1K, Supplementary movie 2). Within the distal OFT, the apposition of the opposing cushions has now created two lateral channels, even prior to fusion of their facing surfaces (Fig. 2, Supplementary Fig. 3). When traced proximally, the channels spiral (Supplementary Figs. 3A,C Movie 3), with the left-sided distal channel moving cranially towards the cavity of the right ventricle, and the right-sided channel directed caudally (Supplementary Figs. 2&3). By this stage, the oblique protrusion from the dorsal wall of the aortic sac (dashed line in Figure 3D; double arrow in Fig 4D) serves to direct the caudal 6th arch arteries towards the left-sided channel, and the cranial 4th arch arteries towards the right-sided channel. Eventual fusion of the protrusion with the distal ends of the cushions closes the space initially existing between these developing aortic and pulmonary channels, thus forming a transient aortopulmonary septum. By analogy to the foramen primum, which exists between the leading edge of the septum primum and the atrioventricular cushions, the space itself can be considered to be the aortopulmonary foramen.

Separation of the distal intrapericardial channels

At the beginning of E11.5, the extrapericardial aortic sac has a cranial part, giving rise to the 4th arch arteries, and a caudal part supporting the 6th arch arteries (Fig. 2G and Movies 4 and 5). The dorsal wall, which separates the arterial orifices, is longer in the mouse compared to man (compare Figs. 3A&B). As discussed above, the space between the dorsal wall and the distal margins of the cushions at this stage is an aortopulmonary (AP) foramen (boxed regions in Fig. 2A-F and circled in H). Analysis of the 25 datasets from E11.5 embryos shows that the foramen closes rapidly during E11.5 (Fig. 2). When viewed externally, the outflow tract and its adjoining pericardial walls are initially smooth (Fig. 4A). Concomitant with bulging of the 6th arch arteries into the pericardial space caudally, and appearance of spiralling counter-clockwise grooves laterally, the latter showing the locations of the eventual separation of the developing intrapericardial aortic and pulmonary trunks (Figs. 4B,C and Movie 6), there is reduction in size of the foramen. Dissections through the OFT reveal formation of a narrow waist caudally, close to the pericardial margins (black arrows in Fig. 4E). Extrapericardially, excavation of the intermediate part of the aortic sac, particularly on the right side, frees the pharyngeal mesenchyme to form the wall of the extrapericardial ascending aorta, which is continuous at the borders of the pericardial cavity with the right-sided non-myocardial tissue derived from the second heart field (Supplementary Fig. 3D and Movies 7-9). Similar processes on the left side form the intra- and extrapericardial parts of the pulmonary trunk (Fig. 5). By the middle of E11.5, the foramen itself is no more than a pinhole (Fig. 3E). The 6th arch arteries, encased within the extrapericardial mesenchyme (Fig. 4D), have also begun to remodel at this stage, with the right 6th arch artery showing marked regression dorsal to the origin of the right pulmonary artery (Supplementary Fig. 2B). Eventual disappearance of this right-sided artery is necessary to achieve full separation of the pulmonary and aortic circuits.

Two populations of NCC close the aortopulmonary foramen

At E9.5 and 10.5, through to early 11.5, the dorsal wall of the aortic sac is predominantly of NCC origin (Figs. 1C,F), overlying a region made up of cells expressing Isl1 (Figs. 5B-D). By this stage, the distal cushions are also filled with NCC (Fig. 5A), which can be traced laterally into the pharyngeal mesenchyme (Fig 1C,F). Fusion of the protrusion with the distal ends of the cushions, each initially covered by an endothelial layer, produces a continuum of NCC (Fig. 2F), albeit with the two populations derived from medial and lateral origins (Fig. 5A). This central structure formed within the distal outflow tract functions transiently as an aortopulmonary septum. Only subsequent to the fusion of the two populations of NCC does it become possible to recognize the condensed whorl-like structure present within the tissues now separating the newly formed intrapericardial aortic and pulmonary channels. This condensed tissue can be traced into the unfused cushions more proximally, where it forms the columns of condensed mesenchyme known as the "prongs"[4,5] (Supplementary Fig. 3). The transient septum formed by fusion of the protrusion and the distal cushions subsequently expresses alpha-smooth muscle actin (aSMA; Fig.5E) and, with ongoing development, its surfaces arterialize to form the adjacent walls of the intrapericardial arterial trunks. The most distal adjacent walls are formed from the surfaces of the protrusion, while the proximal walls are derived from the distal cushions. The core of

the central tissue mass is then replaced by connective tissue (Fig. 5F), so that eventually there is no longer any anatomic septum between the intrapericardial arterial channels.

Different origins of the lateral and facing walls of the intrapericardial arterial trunks

The non-myocardial lateral and distal parts of the developing walls of both the intrapericardial aorta and pulmonary trunk (Fig. 1-I) express Isl1 (Figs 5 B and C), revealing their origin from the second heart field. The adjacent, or facing, walls of these channels, in contrast, do not express Isl1. As described above, being of NCC origin, they are formed distally from the protrusion, and proximally from the distal tips of the cushions (Fig. 5A). The dimple marking the closing aortopulmonary foramen shows the site of union between these two sources of NCC (Fig. 3 F).

Mechanistic insights relating to morphogenesis

If our concept of normal development is correct, malformations related to an abnormal protrusion of the dorsal wall of the aortic sac should be separable from defects caused by failure of fusion of the OFT cushions. With this in mind, we examined mouse models and human specimens, hoping to provide insights to the morphogenesis of lesions such as AP foramen and common arterial trunk. Loop-tail (Lp) mice have a mutation in Vangl2.[6] At E11.5, the pharyngeal region of Lp/Lp embryos shows varying numbers of NCC within the OFT cushions, with uneven distribution of the NCC in the dorsal wall of the aortic sac (Fig. 6A). In some mice, by E12.5, we found that the cushions had fused with each other, forming separate aortic and pulmonary roots, but had failed to fuse with the protrusion, leaving an AP window (Fig 6B,C). Other Lp/Lp mice, in contrast, showed common arterial trunk, with failure of fusion of the outflow cushions, but with separation intrapericardially of the aortic and pulmonary channels due to formation of a dorsal protrusion (Fig. 6D).

Splotch 2H (Sp^{2H}) mice carry a mutation in Pax3, which reduces the population of NCC [7]. At E11.5, there is obvious deficiency of pharyngeal NCC (compare Fig. 6E with 1F and 5A). The dorsal wall of the aortic sac is markedly thinned, with a much reduced population of NCC, and no dorsal protrusion, since the animals also lack sixth aortic arch arteries. By E12.5, the OFT cushions remain unfused (Fig. 6F) and, at later stages, the majority of Sp^{2H}/Sp^{2H} mutants have a common arterial trunk. Deficiency for NCC in the Sp^{2H} mutant, therefore, is associated with failure of fusion of the structures required for separation of the more proximal parts of the OFT, along with absence of the sixth arch arteries, and hence no potential for formation of an aortopulmonary septum.

The malformations seen in the mouse are directly comparable with lesions found in man. The phenotypic feature of human AP windows is the presence of a communication between the intrapericardial arterial trunks, but with normal formation not only of the aortic and pulmonary roots, but also the proximal walls of the intrapericardial arterial trunks (Fig. 6G). This implies failure of closure of the AP foramen, but normal fusion of the outflow cushions. In contrast, the phenotypic feature of human common arterial trunk is the presence of a common arterial valve, indicating a lack of cushion fusion. This is typically seen with the pulmonary arteries arising side-by-side at the margins of the pericardial cavity (Figure 6H), with absence of the sixth arch arteries again meaning that there is no protrusion of the

Europe PMC Funders Author Manuscripts

dorsal wall of the aortic sac. Less frequently, there can be separate intrapericardial aortic and pulmonary channels (Fig. 6I), along with presence of a left sixth arch, suggesting relatively normal formation of the protrusion, but again with overall failure of fusion of the cushions.

Discussion

Numerous hypotheses have been advanced to explain the transformation of the distal part of the developing outflow tract from a channel with a common lumen into the aortic and pulmonary trunks[1]. In some studies [2, 8-10], these changes have been explained on the basis of fusion of an AP septum with the distal ends of the outflow cushions. The structure defined as the AP septum is equivalent to the entity we have described as the protrusion. We prefer to use the term “protrusion” rather than septum for three reasons. First, there is no comparable septal structure in the postnatal heart. Second, it is only the distal half of the embryonic septum between the intrapericardial trunks that is derived from the protrusion, the proximal part being derived from the distal cushions. Third, and perhaps most important, it is more usual nowadays to consider the AP septal complex as separating the intermediate and proximal parts of the outflow tract[11]. The septum, which is a transient structure, cannot be compared to other septums, such as the primary atrial septum, or the muscular interventricular septum, since it does not persist in the postnatal heart. Our three-dimensional reconstructions show clearly how the protrusion forms the dorsal margin of a similarly transient intrapericardial aortopulmonary foramen, subsequently closed by fusion of the protrusion with the distal ends of the cushions. Some authors [4,5,12] have paid scant attention to this contribution made by the dorsal wall of the aortic sac and it is now more customary to consider the AP septum as separating the more proximal parts of the OFT, specifically the arterial roots and the ventricular OFTs.[11] We agree with these findings concerning the role of the cushions as septal structures within the more proximal parts of the OFTs, but this has not been the subject of this current investigation. Rather, we have addressed the formation of the intrapericardial trunks distal to the primordiums of the arterial valves. The AP septal complex as described by the later investigators [4,5,11] does not become evident until after the separation of the intrapericardial arterial trunks. This separation, eventually leading to the formation of discrete adjacent walls for the aorta and pulmonary trunk, also requires marked remodeling and excavation at the junction between the OFT and the aortic sac. This remodeling, not previously described to the best of our knowledge, brings together the developing adjacent walls of the intrapericardial arterial trunks, thus helping to reduce the size of the AP foramen. Another contributing process to separation of the definitive aortic and pulmonary channels, again not previously recognized in this regard, is regression of the dorsal part of the right 6th arch.

The changes we see in our mouse hearts are comparable to those observed in the human heart,[13] albeit also with subtle differences. There is a greater degree of bending of the OFT in man, more obvious formation of the initial non-myocardial spurs seen cranially and caudally at the margins of the pericardial cavity, and a shorter dorsal wall of the aortic sac. The comparable findings in man and mouse, nonetheless, permit us to suggest mechanistic insights not only for normal development, but also for the pathogenesis of lesions such as common arterial trunk and AP window. With regard to normal development, our observations support the important role of NCC in filling the outflow cushions and

separating the more proximal parts of the OFT.[11,12] We also show the importance of a second migration of cells derived from the neural crest, specifically those contained in the protrusion from the dorsal wall of the aortic sac. Thus, we have demonstrated two pathways for migration of NCC into the OFT. Cells migrate laterally to populate the cushions, while others enter medially forming a cap on the part derived from the second heart field. Our findings also confirm the importance of the intrapericardial migrations from the second heart field,[3] our lineage tracing showing that the non-myocardial components derived from the second heart field will form the lateral walls of the intrapericardial trunks, endorsing a similar study in the developing avian heart.[10] The facing walls of the trunks, in contrast, are derived from NCC within the fused protrusion and cushions, while those in the protrusion are supported by a core derived from the second heart field. This core eventually becomes replaced by the connective tissue interposed between the walls of the arterial trunks. Waldo and colleagues[14] had also noted how differing populations of cells formed the distal walls of the arterial trunks, and described circumferential seams between these components. We also envisage the presence of seams between the component parts, but our findings indicate that the seams would extend longitudinally from the sinutubular junctions to the distal margins of the pericardial cavity. Waldo and associates,[14] however, studied the chicken heart, whereas our interpretations are based on findings from the mouse, supported by findings in man.[13]

With regard to the pathogenesis of congenital cardiac malformations, we had suggested previously, in a brief review,[15] that failure to close the embryonic AP foramen would provide a rational explanation for the morphogenesis of AP window. Our current images now provide the detailed evidence underscoring this mechanistic insight, which is further supported by analysis of human hearts with AP windows. The separate nature of the arterial trunks proximal to the window is strong circumstantial evidence supporting our interpretation that the adjacent walls are derived distally from the protrusion, but proximally from the cushions. Our current findings also endorse the concept that failure of fusion of the outflow cushions themselves is responsible for producing common arterial trunk.[16] As already discussed, we fully recognize in this regard the importance of contributions from NCC during normal as opposed to abnormal development,[17] but our findings have shown the duality of these contributions. Both are important in explaining the full spectrum of morphology seen in the setting of common arterial trunk. When seen in humans, common arterial trunks can sometimes show extensive separation of the intrapericardial aortic and pulmonary components. This implies some degree of formation of the intrapericardial protrusion from the aortic sac, a feature also shown in some of our loop-tail mice. This arrangement is termed pulmonary dominance in humans, and is found with either interruption of the aortic arch or severe aortic coarctation, with presence of the arterial duct implying formation of the left sixth arch artery.[18] Common arterial trunk in humans, however, is found most frequently with a predominantly aortic intrapericardial arterial component, the pulmonary arteries typically arising side-by-side from the dorsal part of the trunk,[18] and with no formation of any distal aortopulmonary septal structure in absence of any sixth arch arteries. The pathogenesis of malformations involving the intrapericardial arterial trunks, therefore, involves processes that reduce the intrapericardial protrusion of the dorsal wall of the aortic sac and requires failure of fusion of the outflow cushions, or a

combination of these events, these mechanistic insights only being understandable on the basis of normal development as currently described.

Supplementary Material

Refer to Web version on PubMed Central for supplementary material.

Acknowledgments

We are indebted to Professor Susan Lindsay, and the staff of the Newcastle MRC-Wellcome Human Developmental Biology Resource, for providing the human embryos for episcopic examination.

Funding Sources: This work was supported by British Heart Foundation Programme grants RG/03/012 and RG/07/007; European Commission FP6 Integrated Project Heart Failure and Repair, Contract No. 018630; FP7 Collaborative project 261057 European Network for Translational Research in Atrial Fibrillation; and the Medical Research Council UK (U117562103).

References

1. Okamoto N, Akimoto N, Hidaka N, Shoji S, Sumida H. Formal genesis of the outflow tracts of the heart revisited: Previous works in the light of recent observations. Congenit Anom. 2010; 59:141–158.
2. Kramer TC. The partitioning of the truncus and conus and the formation of the membranous portion of the interventricular septum in the human heart. Am J Anat. 1942; 71:343–370.
3. Waldo KL, Kumiski DH, Wallis KT, Stadt HA, Hutson MR, Platt DH, et al. Conotruncal myocardium arises from a secondary heart field. Development. 2001; 128:3179–3188. [PubMed: 11688566]
4. Kirby ML, Gale TF, Stewart DE. Neural crest cells contribute to normal aorticopulmonary septation. Science. 1983; 220:1059–1051. [PubMed: 6844926]
5. Bartelings MM, Gittenberger-de Groot AC. The outflow tract of the heart-embryologic and morphologic correlations. Int J Cardiol. 1989; 22:289–300. [PubMed: 2651326]
6. Henderson DJ, Conway SJ, Greene ND, Gerrelli D, Murdoch JN, Anderson RH, et al. Cardiovascular defects associated with abnormalities in midline development in the Loop-tail mouse mutant. Circ Res. 2001; 89:6–12. [PubMed: 11440971]
7. Conway SJ, Henderson DJ, Copp AJ. Pax3 is required for cardiac neural crest migration in the mouse: evidence from the splotch (Sp2H) mutant. Development. 1997; 124(2):505–514. [PubMed: 9053326]
8. Van Mierop LHS, Alley RD, Kausel HW, Stranahan A. Embryology of the ventricles and great arteries. Am J Cardiol. 1963; 12:216–225. [PubMed: 14047494]
9. Orts-Llorca F, Puerta Fonella J, Sobrado J. The formation, septation and fate of the truncus arteriosus in man. J Anat. 1982; 134:41–56. [PubMed: 7076544]
10. Waldo K, Miyagawa-Tomita S, Kumiski D, Kirby ML. Cardiac neural crest cells provide new insight into septation of the cardiac outflow tract: aortic sac to ventricular septal closure. Dev Biol. 1998; 196(2):129–144. [PubMed: 9576827]
11. Thompson RP, Sumida H, Abercrombie V, Satow Y, Fitzharris TP, Okamoto N. Morphogenesis of human outflow tract. Anat Rec. 1985; 213:578–586. 538–9. [PubMed: 4083538]
12. Kirby, ML. Neural crest, great arteries, and outflow septation. In: Kirby, ML., editor. Cardiac Development. Oxford University Press; Oxford: 2007. p. 143-160.
13. Sizarov A, Anderson RH, Mohun TJ, Brown NA, Lamers WH, Moorman AFM. Three-dimensional and Molecular Analysis of the Arterial Pole of the Developing Human Heart. J Anat. 2012; 220:336–349. [PubMed: 22296102]
14. Waldo KL, Hutson MR, Ward CC, Zdanowicz M, Stadt HA, Kumiski D, et al. Secondary heart field contributes myocardium and smooth muscle to the arterial pole of the developing heart. Dev Biol. 2005; 281:78–90. [PubMed: 15848390]

15. Anderson RH, Cook A, Brown NA, Henderson DJ, Chaudhry B, Mohun T. Development of the outflow tracts with reference to aortopulmonary windows and aortoventricular tunnels. Cardiol Young. 2010; 20(Suppl 3):92–99. [PubMed: 21087564]
16. Van Mierop LHS, Patterson DF, Schnarr WR. Pathogenesis of persistent truncus arteriosus in light of observations made in a dog embryo with the anomaly. Am J Cardiol. 1978; 41:755–762. [PubMed: 645581]
17. Nishibatake M, Kirby ML, Van Mierop LH. Pathogenesis of persistent truncus arteriosus and dextroposed aorta in the chick embryo after neural crest ablation. Circulation. 1987; 75:255–264. [PubMed: 3791607]
18. Russell HM, Jacobs ML, Anderson RH, Mavroudis C, Spicer D, Corcrain E, et al. A simplified categorization for common arterial trunk. J Thorac Cardiovasc Surg. 2011; 141:645–653. [PubMed: 20965518]

Europe PMC Funders Author Manuscripts

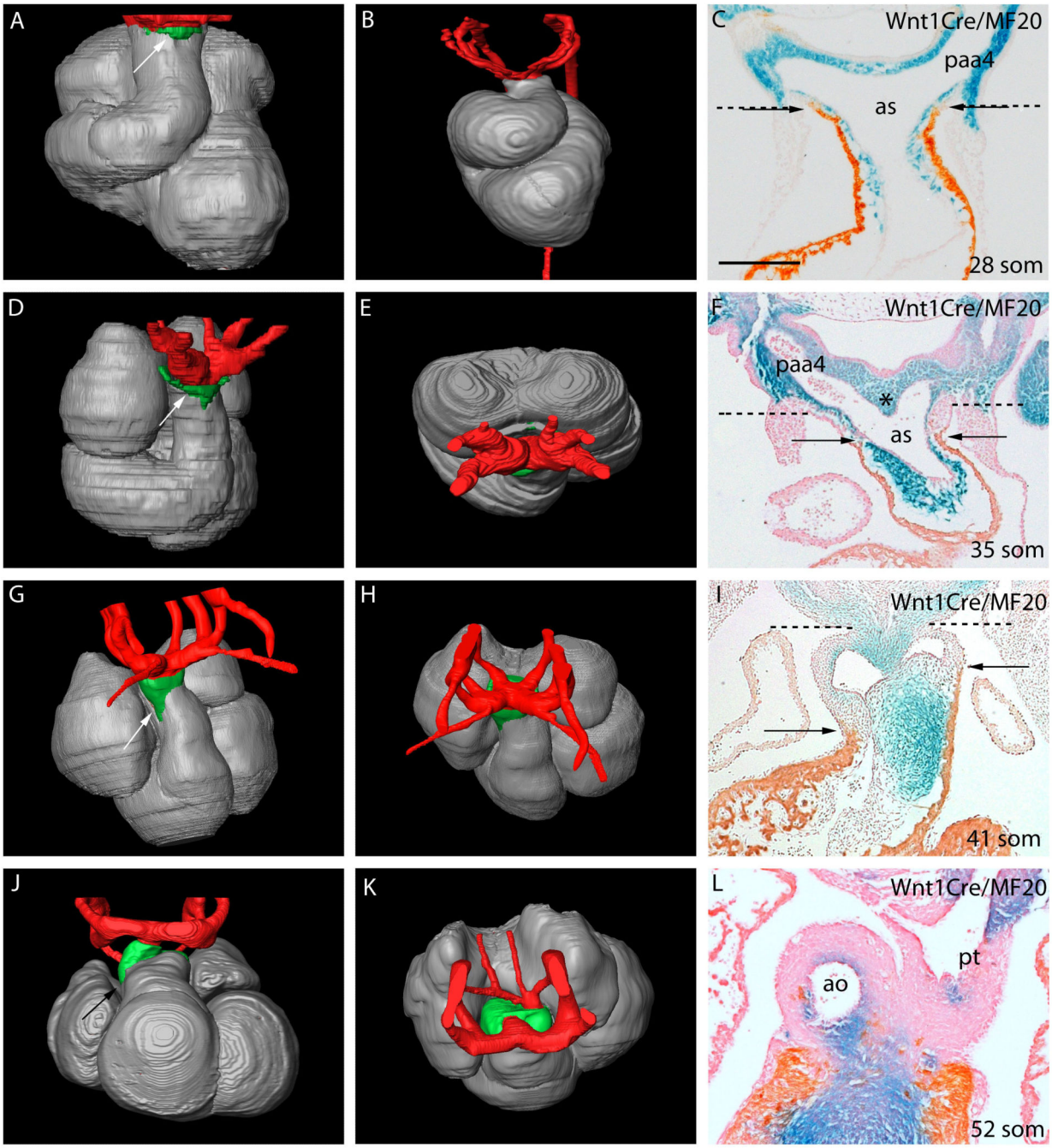

Figure 1. Changes occurring in the composition of the developing mouse (A,C-L) and human (B) OFT, as revealed by Amira reconstructions.

Extrapericardial aortic arch arteries are labeled in red, myocardium in silver, and the non-myocardial intrapericardial mural components in green. The images on the right are from Wnt1-cre;R26R embryos, with NCC stained blue. In C,F,I,L the myocardium is labeled orange/brown by the MF20 antibody. The dashed lines in C,F,I show the level of the pericardial reflections, with the non-myocardial lateral walls of the distal outflow between the dashed lines and arrows. Supplementary Movie 2 shows animated sequences illustrating the arrangement of the aortic arch arteries comparable to the stages shown.

A,C=28somites, B=CS12, D-F=35 somites, H-I=41 somites, J-L=52 somites.
Scale bar in: C=410μm, F=500μm, I=620μm, L=630μm.
ao=aorta; as=aortic sac; paa4=fourth pharyngeal arch artery; pt=pulmonary trunk.

Europe PMC Funders Author Manuscripts

Europe PMC Funders Author Manuscripts

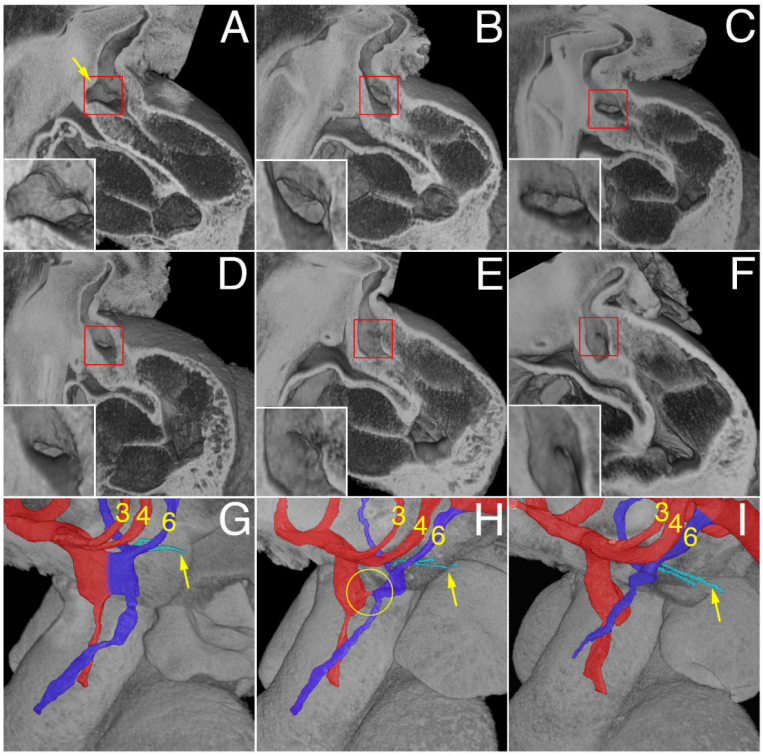

Figure 2.

A-F) Episcopic images showing the reduction is size and eventual closure of the AP foramen in E11.5 mouse hearts. All are shown from the right side, having removed the parietal wall of the cardiac structures. The insets show the foramen in detail. The arrow in panel A marks the protrusion of the dorsal wall of the aortic sac. G-I) Show the remodeling of the junction of the OFT with the aortic sac, comparing early (G), middle (H) and late (I) stages of E11.5. The developing aortic channel is shown in red, along with the third and fourth arch arteries, while the pulmonary channel and sixth arch arteries are shown in deep blue, with the pulmonary arteries arrowed. The circle in H shows the closing aortopulmonary foramen.

Europe PMC Funders Author Manuscripts

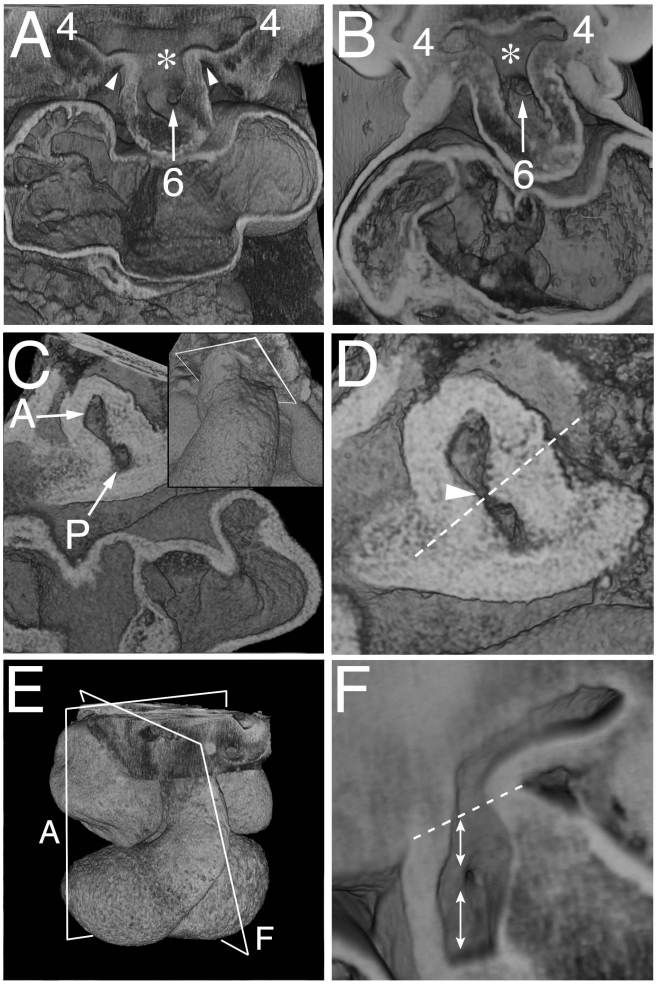

Figure 3. Episcopic images showing the rotation of the boundary of the distal OFT with the pharyngeal mesenchyme.

A) Shows the aortic sac with cranial and caudal components at early E11.5, which give rise symmetrically to the fourth and sixth arch arteries, respectively. The asterisk shows the intermediate part of the sac, with the dorsal wall separating the systemic and pulmonary parts of the sac. B) Is from a CS14 human embryo showing a comparable arrangement. C,D) Show views of a mid E11.5 OFT cut transversely through the closing AP foramen (arrow in D), close to the aortic sac, as shown in the inset in C. The oblique orientation of the protruding dorsal wall of the aortic sac is shown as the dashed line in D. E) Is an over view of an E11.5 heart, showing the orientation of section of A and F. F) Is a view made by removing the parietal wall of the aorta, as in Fig 2F, just prior to closure of the AP foramen. The dotted line shows the border between the intra- and extrapericardial aortic components. The upper double headed arrow shows the walls distal to the foramen, derived from the protrusion, while the lower double headed arrow shows the adjacent wall of the aorta proximal to the foramen, derived from the fused distal cushions.

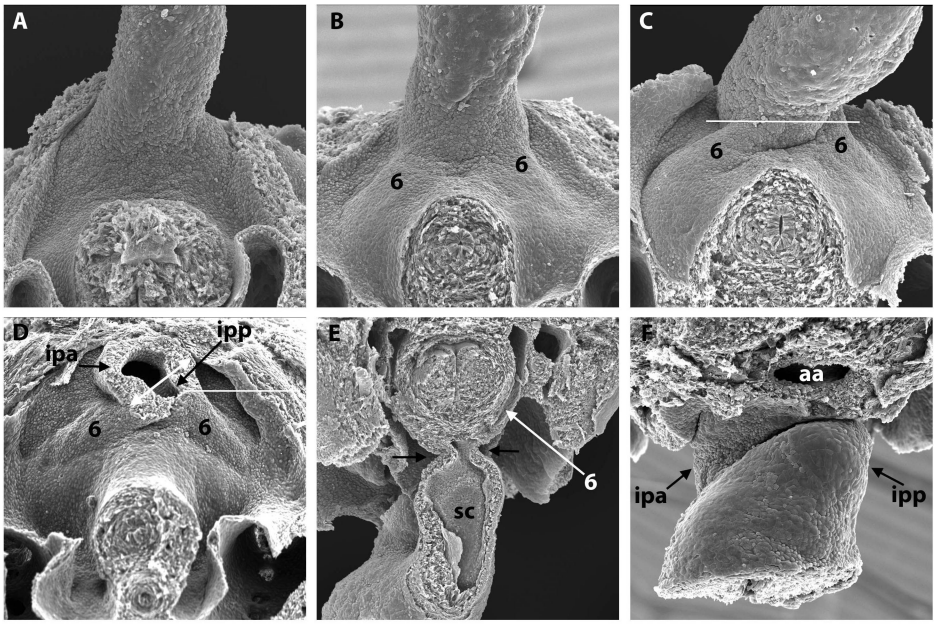

Figure 4. Scanning electron micrographs of E10.5 and 11.5 mouse embryos.

A) (E10.5) and B-D) (E11.5) show the junction of the OFT and the mediastinal wall, viewed inferiorly, with the transected foregut and bilateral cardinal veins visible beneath. Note the progressive asymmetric bulging of the left and right 6th aortic arches (labelled 6 in B,C,D,E) into the pericardial cavity. This, together with excavation at the pericardial border, gives the impression that the OFT is being twisted anticlockwise in this ventral view. In D), the OFT has been transected in the plane indicated by the white line in C. This shows that the lumen at the site of the cut is made up of a large right-sided cranial portion that will be the intrapericadial aorta (ipa), and a small left-sided caudal portion that will be the pulmonary trunk (ipp). The double-headed white arrow shows the oblique orientation of the AP foramen and the protrusion. E) shows an OFT that has been sectioned longitudionally (transverse to the embryo, at the level shown by the white line in D) and is viewed superiorly. Note the narrowness of the junction (arrows) between OFT and body. The septal cushion (SC) is visible in the inferior portion of the OFT. F) shows a late E11.5 junction of the OFT and the mediastinal wall, viewed superiorly, showing the pronounced remolding between the ipa and ipp.

aa – aortic arch.

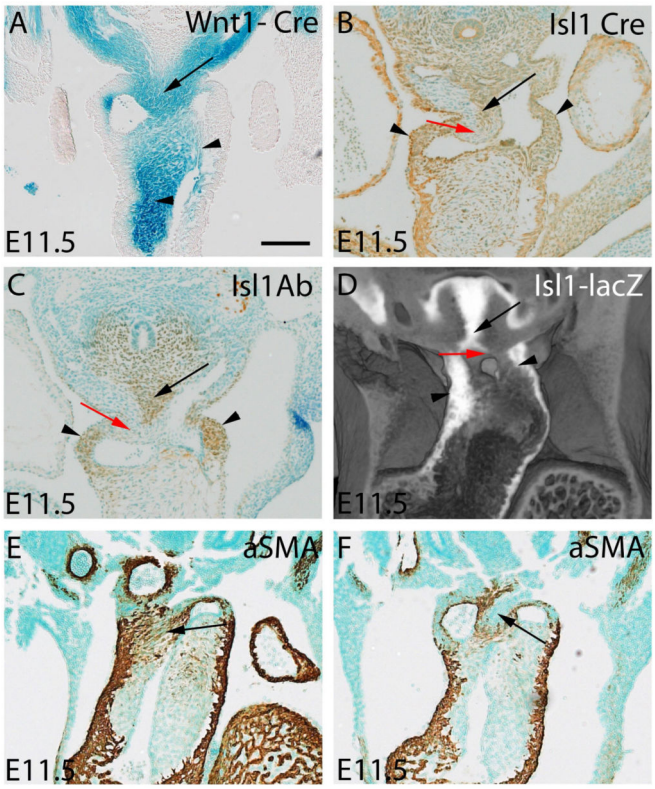

Figure 5. The panels show the lineage of the components involved in separating the initially common lumen of the distal OFT.

A-D) are mid-E11.5, while E,F) are late E11.5. A) shows NCC stained blue from a Wnt1-cre;R26R embryo. The upper arrow shows the cells in the ventral protrusion, while the lower arrows show the NCC in the cushions. B,C) show a section stained for Isl1 antibody, and a comparable section from an Isl1cre;R26EYFP embryo. The brown tissues show the Isl1-positive non-myocardial parietal tongues (small arrows) and the ventral protrusion (long arrow). The surface of the protrusion is negative for Isl1, but as shown in panel A, is positive for NCC. D) shows an episcopic dataset reconstructed from an Isl1-lacZ reporter embryo, illustrating the same features, with the surface of the protrusion shown by the red arrow. E,F have been stained using an aSMA antibody. In E, the fusion site of protrusion and cushions has arterialized, forming the site of the so-called whorl (arrow). At a slightly later stage, as seen in F, the surface of the protrusion remains aSMA positive, but the core of the protrusion is negative, being replaced by connective tissue between the developing adjacent walls of the intrapericardial arterial trunks (arrow).

Scale bar represents: A=950μm, B,C=1040μm, E,F=815 μm

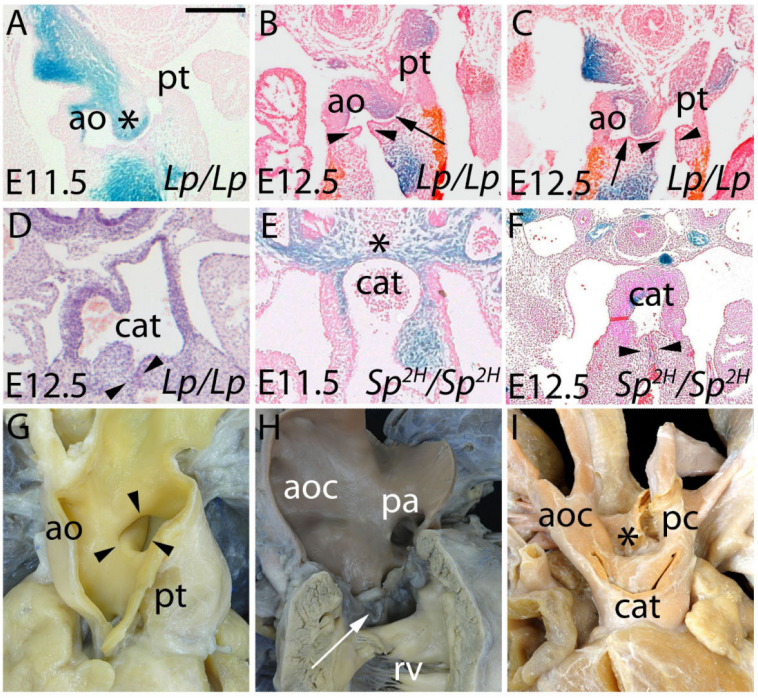

Figure 6. The panels compare the situation in mouse mutants (A-F) with human hearts showing AP window (apw – G) and common arterial trunk (cat - H,I).

Lp/Lp are shown in A-D, Sp^{2H}/Sp^{2H} in E,F. A) shows formation of the ventral protrusion in an E11.5 Lp/Lp (asterisk), but failure of fusion of the protrusion with the cushions. B,C) show an AP window, with separate formation of aortic (ao) and pulmonary (pt) valvar leaflets (arrowheads). The arrow shows the AP window. D) shows common arterial trunk, but with obvious separation of the intrapericardial aortic and pulmonary components. In E,F), the Sp^{2H}/Sp^{2H} have common arterial trunk, with absence of any protrusion of the dorsal wall of the aortic sac in E. The arrows in F show the forming valves. G) shows an AP window in a human seen through the aorta (ao). Note the separate channels of the aorta and pulmonary trunk (pt) proximal to the window. In the common arterial trunk shown in H (arrow) there is no separation of the intrapericardial trunk, which is essentially aortic (aoc), the pulmonary arteries (pa) arising from the leftward and dorsal part of the trunk. The heart in I), in contrast, has separate formation of the intrapericardial aortic and pulmonary components (aoc, pc), with the pulmonary component continuing to supply the descending aorta through a persistently patent arterial duct.

Scale bar represents: A,E=770μm, B,C =455μm, D=500 μm, F=400μm.